

# RSC Advances



This is an *Accepted Manuscript*, which has been through the Royal Society of Chemistry peer review process and has been accepted for publication.

*Accepted Manuscripts* are published online shortly after acceptance, before technical editing, formatting and proof reading. Using this free service, authors can make their results available to the community, in citable form, before we publish the edited article. This *Accepted Manuscript* will be replaced by the edited, formatted and paginated article as soon as this is available.

You can find more information about *Accepted Manuscripts* in the [Information for Authors](#).

Please note that technical editing may introduce minor changes to the text and/or graphics, which may alter content. The journal's standard [Terms & Conditions](#) and the [Ethical guidelines](#) still apply. In no event shall the Royal Society of Chemistry be held responsible for any errors or omissions in this *Accepted Manuscript* or any consequences arising from the use of any information it contains.

# Improvement on optical modulation and stability of the NiO based electrochromic devices by nanocrystalline modified nanocomb hybrid structure

Xin Zhang, Yongzhe Zhang\*, Bowen Zhao, Shujuan Lu, Hao Wang, Jingbing Liu, Hui Yan

*The College of Materials Science and Engineering, Beijing University of Technology, Beijing, 100124, P.R. China*

**Abstract:** Among the explored materials for electrochromic devices (ECDs), nickel oxides thin films have been widely applied as an optical anodic layer due to its adjusting optical property by ions exchanging. Generally, to realize the three important characters including color contrast, switch speed and cycling durability, it requires the electrochromic layer own different microstructures or crystalline properties. Thus it is still a difficulty to design a suitable structure for NiO film to own excellent electrochromic performance. Here, a nanocrystalline modified nanocomb novel NiO structure is prepared by a simple chemical process. This novel microstructure shows highly multiple channels, high surface areas and good crystalline. All of these characters produce a good electrochromic performance including fast switch speed (around 2s), high color contrast (69.4%) and in company with good cycling durability (more than 1000 cycles). This simple chemical process demonstrated here could be suitable for the large scale production for the future electrochromic devices application.

**Keywords:** NiO; Electrochromic; Chemical bath deposition; Nanoparticle

\* **Corresponding author:** The College of Materials Science and Engineering, Beijing University of Technology, Beijing 100124, P. R. China. E-mail: [yzzhang@bjut.edu.cn](mailto:yzzhang@bjut.edu.cn); Tel: +86-10-6739-1061

## Introduction

Electrochromic devices (ECDs) change optical modulations during electrochemical oxidation/reduction through ion insertion/ extraction which is induced by the application of low electric voltage<sup>1, 2</sup>. They have attracted much attention in recent years due to they can be applied to large area displays, smart mirrors, smart windows and military camouflage<sup>3, 4</sup>. ECDs based on a multilayer films construction consists of transparent conducting layer, electrochromic layer, ion conducting layer and ion storage layer.<sup>5</sup> NiO is an attractive electrochromic material because of its low power consumption and stable memory effect under open circuit conditions, which can be used as ion storage layer in ECDs in recent years<sup>5-7</sup>. Nevertheless, low color contrast, slow switching speed and poor cycling stability have restricted the commercial exploitation of the NiO electrochromic film<sup>8, 9</sup>. Up to now, the NiO films with different nanostructures have been synthesized by a variety of methods, such as vacuum evaporation<sup>6</sup>, electrodeposition process<sup>10</sup>, pulsed laser deposition<sup>11</sup>, spray pyrolysis<sup>12</sup>, sol - gel process<sup>13</sup>, and chemical bath deposition (CBD)<sup>3</sup>, etc. It is well accepted that color contrast highly related to the active surface area of the electrochromic materials. Generally, NiO films with large surface area possess much more active reaction area and then lead to higher color contrast<sup>8</sup>. Xia et al.<sup>14</sup> have investigated the effect of morphology on the electrochromic and electrochemical performances of the NiO films. The results showed that highly porous NiO film exhibited much better electrochromism (transmittance up to 82% at 550 nm) than the smoothly compact sol-gel NiO film. For the switch speed, it is known that electrochromic process is associated with double injection (extraction) of ions and electrons to (from) the electrochromic film. In contrast to the usual nanoparticle and nanorod structures, the porous NiO nanowall structures exhibit more capillary pathways for the ion intercalation and deintercalation<sup>13</sup>. Furthermore, migration of ions will be promoted and consequently redox reactions will become faster if the capillary pathways of the electrochromic materials increases<sup>4</sup>. Cao et al. compared the electrochemical and electrochromic performances of mesoporous NiO nanowall arrays film and dense NiO film<sup>7</sup>. The mesoporous NiO nanowall arrays film

possessed fast switching speed (2 s for coloration and 2.5 s for bleaching), which was better than the dense NiO film (4 s for coloration and 4.5 s for bleaching). The cycling stability is also an important factor in device applications, for instance a well cycling stability is necessary in smart windows or display device<sup>9</sup>. It is generally acknowledged that most of the NiO films suffer from poor cycling stability due to structure disintegration or strain induced by injection or extraction of ions<sup>15</sup>. Zhang et al. synthesized Co-doped NiO nanoflake array electrochromic films which could reduce internal strain and accommodate the vast volume changes<sup>15</sup>. Moreover, Cai et al. synthesized NiO nanoparticles film by a solvothermal method, and the uniform NiO granules grew on the ITO glass substrates<sup>8</sup>. The NiO nanoparticles electrodes exhibit excellent reaction stability which sustained a transmittance modulation of about 56.4% even when subjected to 5000 cycles. It indicates that the excellent electrochemical performance might be attributed to the uniform nanoparticles morphology and stable chemical bonding of NiO nanoparticles which could stop from the structure disintegration on the substrates. Although the EC performances are enhanced for some aspects, as for the porous NiO nanowall film prepared by CBD, cyclic stability is still the major unsolved problems<sup>3</sup>. Xia et al. used CBD method in combination with a heat-treatment process to prepare porous net-like NiO films<sup>3</sup>. The intercrossing network exhibits higher surface area and provides much more pathways for the double intercalation (deintercalation) of ions and electrons to (from) the film. The porous NiO thin film shows excellent electrochemical and electrochromic properties which optical modulation up to 82%. However, part of film peeled off from the ITO substrate after 300 cycles and hardly switched from brown to transparent.

Above all, for the three important characters in ECD, color contrast, switch speed and cycling durability, it requires that the electrochromic layer own different microstructures or crystalline properties. Therefore, to achieve excellent electrochromic performances, it still needs careful microstructure design and then fabricate high-quality electrode materials. Here, a novel hybrid NiO film (NH-film) was carefully designed, where nanocrystalline was modified on NiO nanocomb by a chemical process. Comparing with CBD NiO film (CBD-film) and NiO nanoparticles film (N-film), the NH-film exhibits larger optical modulation, relatively faster

electrochromic response time and longer cycle life.

In addition, this simple chemical process demonstrated here could be suitable for the large scale production for the future electrochromic devices application.

## 2. Experimental section

### 2.1 Preparation of different NiO films.

All the chemical reagents were analytical grade, and used as received without any further purification. All aqueous solutions were prepared using ultra pure water. Nickel sulfate, potassium persulfate, aqueous ammonia, acetone, n-hexane and methyl alcohol were bought from Tianjin Fuchen Chemical Reagents Factory. Hexane suspension, oleylamine were bought from Aladdin. ITO substrates were produced by Zhuhai Kaivo Optoelectronic Technology Co., Ltd.

The CBD NiO film was synthesized following a CBD approach<sup>3</sup>. Firstly, 80 ml of 1M nickel sulfate (Tianjin Fuchen Chemical Reagents Factory), 60 ml of 0.25 M potassium persulfate and 20 ml of aqueous ammonia (25-28% NH<sub>3</sub>) were mixed in a 250 ml pyrex beaker at room temperature to obtain CBD solution. To prevent deposition on the nonconductive sides, indium tin oxide (ITO, cleaned using acetone, ethanol, and deionized water, sequentially) substrate was masked with polyimide tape. Then the ITO substrate was vertically placed in the obtained CBD solution, and kept at room temperature for 30 min under constant vigorous stirring to precipitate the precursor film. The precursor film was washed with deionized water and removed the tape mask, then dried at 60 °C. Finally, the as prepared precursor was annealed at 400 °C for 2 h.

The NiO nanoparticles suspended in hexane suspension were synthesized through a thermal injection method<sup>16</sup>. In a typical synthesis, 1 mmol nickel nitrate and 1 ml oleic acid were mixed with 5 ml of methyl alcohol, then the solution was injected into 25 ml oleylamine at temperature of 180 °C and mixture was heated to 300 °C for an hour under an argon atmosphere. After cooling to room temperature, 50ml acetone was added to precipitate the NiO nanoparticles. Then the dispersion was centrifuged at a revolving speed of 11000r/d and then dispersed into n-hexane to prepare N-film. The N-film was prepared by dip coating method. Afterwards, the film was dried in air at 60 °C, and then annealed at 400 °C for 2 h.

The as deposited precursor film obtained by CBD method was used as the substrate of NH-film. In the second step, the combination of the NiO nanoparticles was obtained by dip coating method. After that, the precursor was dried in air at

60 °C, and then annealed at 400 °C for 2 h. The thickness of the film was approximately 500 nm determined with an Alpha-step 200 profilometry.

## 2.2 Characterization of structure and morphology

The X-ray diffraction (XRD) patterns of powders scratched from NiO films with different nanostructures were carried out on a Shimadzu XRD diffractometer using Cu K $\alpha$  radiation. The morphologies and microstructures of films were observed using field emission scanning electron microscopy (FESEM, Hitachi, S-4800) and transmission electron microscopy (TEM, JEM 2100). Data of N<sub>2</sub> physisorption analysis BET specific surface areas were carried out by Micromeritics TriStar II 3020 Surface Area and Porosity apparatus.

## 2.3 Electrochromic and electrochemical measurements

To investigate the electrochromic behavior of NiO films with different nanostructures, the transmission spectra of samples in the colored and bleached states were measured over the range from 300 to 1000 nm with a Shimadzu UV-3101PC spectrophotometer.

The electrochemical measurements were carried out by a conventional three-electrode system using 1M KOH aqueous solution as the electrolyte. Cyclic voltammetry (CV) and chronoamperometry (CA) measurements were performed on a Princeton VersaSTAT 4 electrochemical workstation. Different NiO samples worked as the working electrode, platinum foil and an Ag/AgCl electrode were employed as the counter electrode and reference electrodes, respectively.

## 3 Results and discussions

### 3.1 Morphology and structure of NiO films

The morphologies and microstructures of NiO films with different nanostructures are shown in Fig. 1. The CBD NiO film exhibits a highly porous net-like structure made up of many interconnected nanowalls (Fig. 1a-b). Most of the nanowalls are nearly vertical, and the average thickness of the walls has been estimated as 20 nm. From Fig. 1c and 1d, it can be obviously seen that the N-film prepared by dip coating method exhibits a dense surface morphology consisted of lots of NiO nanoparticles of 10 nm. Fig. 1e and 1f show the SEM images of the NH-film. The porous net-like structure of the NH-film possessed much capillary pathways for the ion intercalation and deintercalation. The existence of NiO nanoparticles can be distinctly seen over the surface of the nanowalls. In addition, the NiO nanoparticles homogeneously adhered to the surface of the nanowalls and clustered over the substrate of porous CBD NiO in

NH-film.

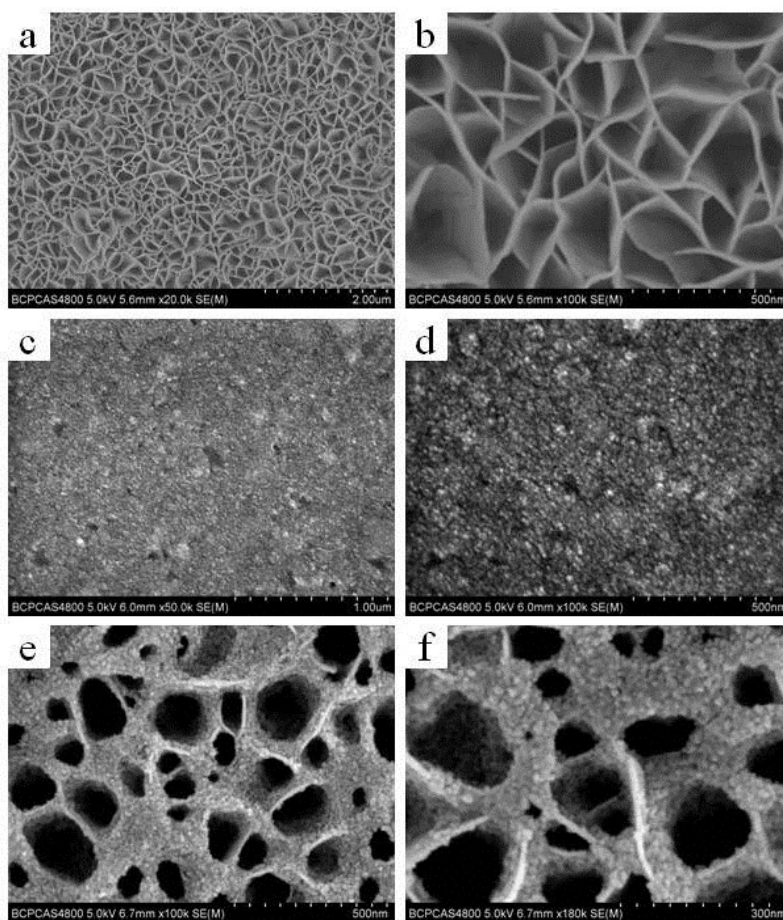


**Fig. 1** SEM micrographs: (a) - (b) CBD film, (c) - (d) N-film, (e) - (f) NH-film.

Further insights into the microstructural characteristics of NiO films scratched from the ITO substrate are investigated by TEM, as shown in Fig. 2. The CBD NiO film exhibits unique features composed of nanosheets structures (Fig. 2a). The N-film consisted of uniform granules possessing an average diameter of 10 nm. In contrast, the NH-film possesses a characteristic morphology with nanosheets covered by NiO nanoparticles, the uniform granules which adhered to the surface of the nanowalls possess an average diameter around 10 nm. The NH-film exhibits with large surface area, this is in good consistency with SEM results.

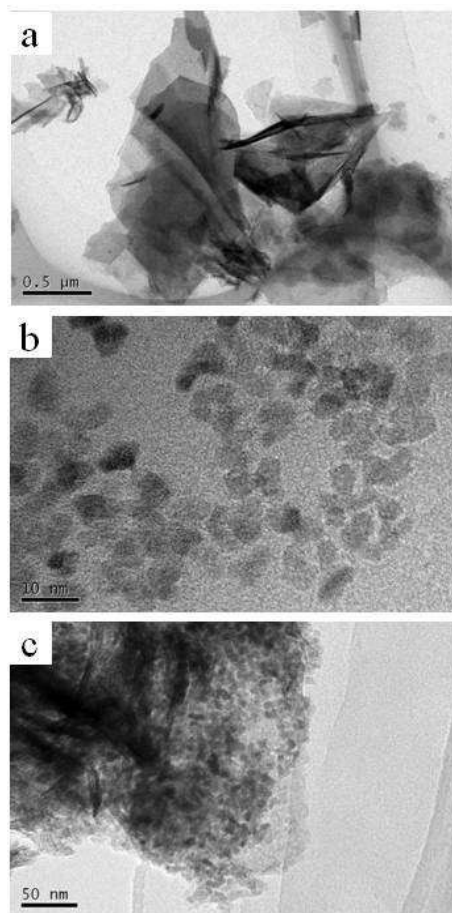


**Fig. 2** TEM micrographs of (a) CBD film (b) N-film (c) NH-film.

BET specific surface areas were carried out by Micromeritics TriStar II 3020 Surface Area and Porosity apparatus. The BET specific surface area of the CBD film and NH-film were high up to  $113.95 \text{ m}^2/\text{g}$  and  $84.74 \text{ m}^2/\text{g}$ , respectively. While, the BET specific surface area of the N-film is  $9.33 \text{ m}^2/\text{g}$ . That the diminutive BET specific surface area of the N-film may be resulted from the aggregation of the NiO nanoparticles. The nitrogen adsorption–desorption isotherms of the samples are shown in Fig. 3 (a). The three samples show different isotherms indicating that different pore structures were formed. The CBD film and NH-film samples have similar hysteresis, which appear in the high relative pressure range of 0.47–1.0. This hysteresis loop is of type H3, indicating a broad pore distribution in the macropore range. Its corresponding pore size distribution is shown in Fig. 3 (b), the CBD film centered at 126 nm, the NH-film centered at 80 nm. The total pore volumes of pores of CBD at  $P/P_0 = 0.99$  is  $0.202627 \text{ cm}^3/\text{g}$  and NH-film is  $0.189787 \text{ cm}^3/\text{g}$  respectively. Compared to the CBD film and NH-film samples, the pore size in the N-film is

smaller and the pore size distribution is narrower, which is a typical trend of mesoporous materials with uniform pore systems. This is confirmed by the pore size distribution curve, where an exactly uniform pore size distribution centered at 3.2 nm was found, as shown in Fig. 3 (b). And the total pore volume of pores at  $P/P_0 = 0.99$  is  $0.009679 \text{ cm}^3/\text{g}$ . These are in good consistency with SEM and TEM results.

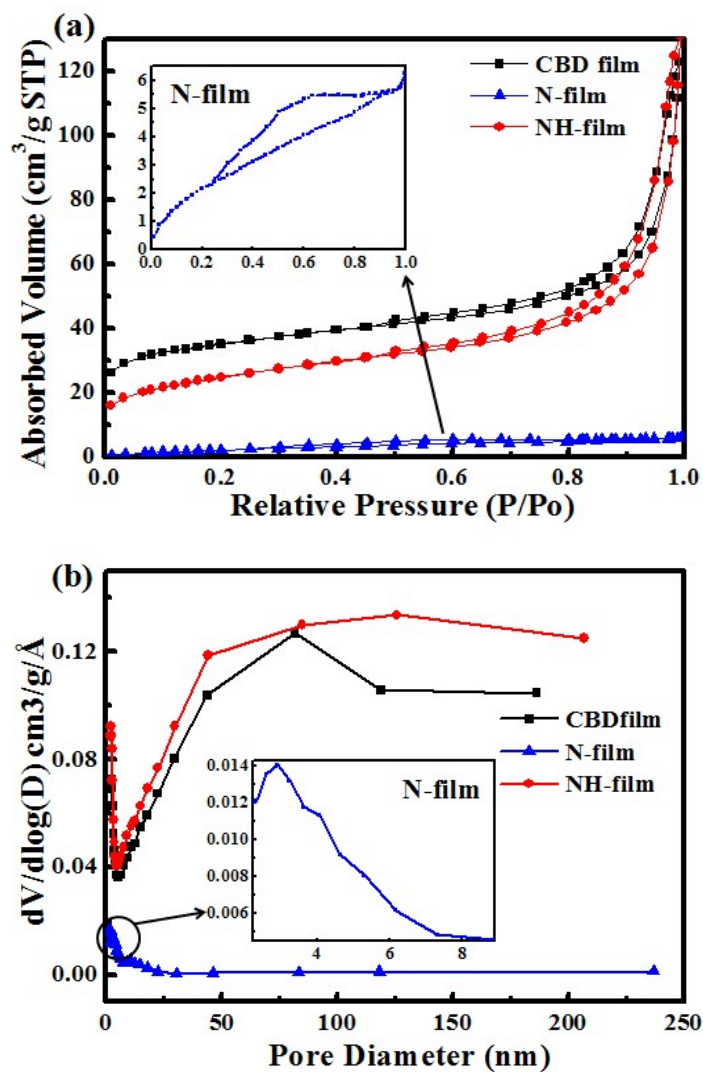


**Fig. 3** (a) Nitrogen adsorption–desorption isotherms and (b) BJH pore-size distribution of NiO power scratched from different films.

Fig. 4 presents the XRD patterns of the powders scratched from NiO films with different microstructures. The typical peaks of cubic NiO phase (JCPDS 4-0835) can be found in Fig. 4, indicating the formation of NiO after heat treatment. Additionally, the crystallite size of NiO is calculated using the Debye-Scherrer equation as follows:

$$D = 0.89\lambda/B\cos\theta \quad (1)$$

Where  $D$  is the size of crystallite,  $B$  is the broadening of diffraction line measured at half of its maximum intensity and  $\lambda$  is the wavelength of X-rays ( $1.5405\text{\AA}$ ),  $\theta$  is the diffraction angle. The average particle size of CBD film is calculated to be 6 nm. As for the N-film and NH-film, the particle sizes were 11 nm and 8 nm, respectively.

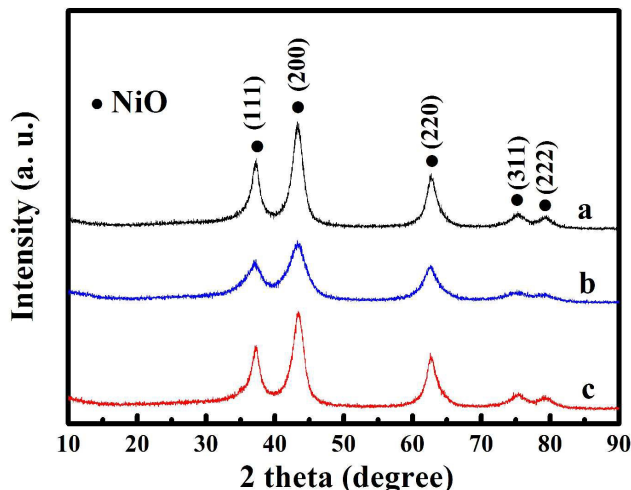


Fig. 4 XRD patterns of powders from (a) CBD film, (b) N-film, (c) NH-film.

### 3.2 Electrochromic and electrochemical performance

The electrochromic properties of NiO films with different nanostructures were investigated after the film electrodes had been subjected to CV test for 10 cycles in 1 M KOH solution in order to stabilize the redox reactions. The NiO film electrodes were colored to dark brown (colored state) by applying step voltages of 0.8 V, and -0.8 V (vs. Hg/HgO) was applied for bleaching to neutral transparent (bleached state). Fig. 5 presents the optical transmittance of NiO films with different nanostructures in colored and bleached states. It is clearly seen that the NH-NiO film presents a more noticeable transmittance modulation ( $\Delta T$ ) than the other two films. The  $\Delta T$  of the NH-film between colored and bleached states is high up to 69.4 % at 550 nm. While the  $\Delta T$  of the CBD film and N-film were 62.9 % and 43.3 %, respectively. It clearly reveals that the combination of NiO nanoparticles promoted transmittance variation of the NH-film.

The optical density change ( $\Delta OD$ ) can be defined by:

$$\Delta OD = \log(T_b/T_c) \quad (2)$$

where  $T_b$  and  $T_c$  are the transmittance of the bleached state and colored state at 550 nm, respectively<sup>17</sup>. Table 1 illustrates the  $\Delta OD$  of different NiO films acquired from Fig. 5. The  $\Delta OD$  of the NH-film is 0.90, which is larger than those of CBD NiO film (0.64) and N-film (0.45), suggesting that the NH-film possesses good color contrast.

The properties of the NiO films correspond to the structure and surface topography<sup>7,18</sup>. It is universally acknowledged that electrochromic process is an electrochemical reaction associated with double insertion (extraction) of ions and electrons to (from) the electrochromic film<sup>3</sup>. NiO films with large surface area possess much more active reaction area and lead to higher color contrast<sup>14</sup>. Compared with the CBD NiO film and N-film, the NH-film was filled with NiO nanoparticles. The NiO nanoparticles which filled in the multiholes not only increased the electrochromic active sites, but also held large reaction surface and capillary pathways. All these contributed to the improvement of electrochromic performance.

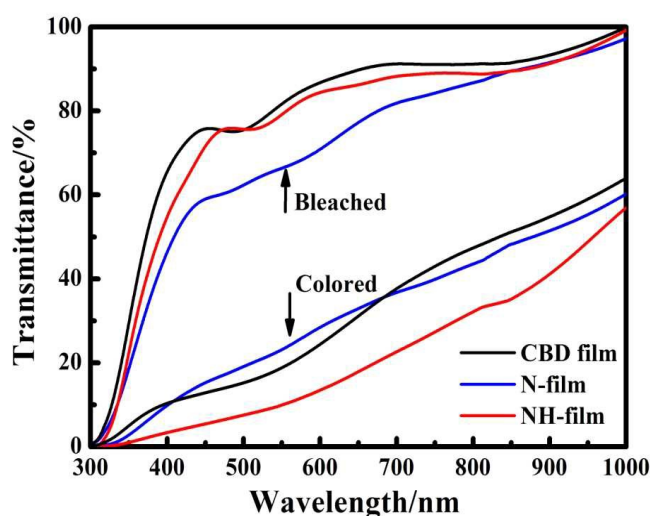


**Fig. 5** Optical transmittance spectra of NiO films prepared by different methods annealed at 400°C at the 10st potential cycles.

Fig.6 shows the photographs of NiO thin film on the bleached and colored states. The bleached state of composite NiO film is very transparent so that pictures of background can be seen clearly. In contrast, it changes to brownish black when it is in colored state.

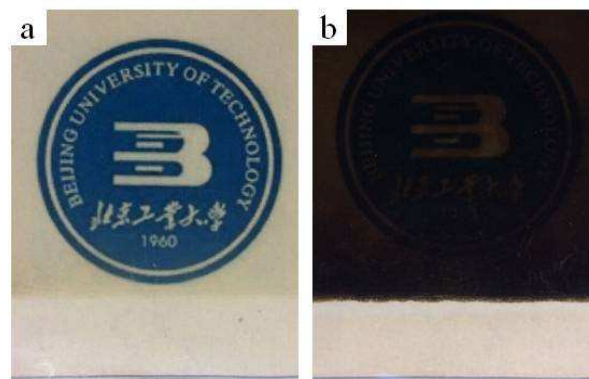


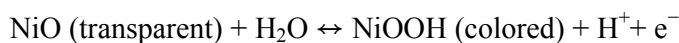
**Fig. 6** Photographs of a sample with a size of  $2.5 \times 2.5 \text{ cm}^2$  in the (a) bleached and (b) colored states.

The electrochemical behaviors of different NiO thin films were investigated by CV, CA and coloration-bleaching cycling tests. Fig. 7 compares the CV curves of different NiO films which were recorded at the 10th cycle in a 1 M KOH electrolyte. The scanning potential region was from  $-0.8\text{V}$  to  $+0.8\text{V}$  at a scan rate of  $50 \text{ mVs}^{-1}$ . During the CV curves, the oxidation peak is associated with the intercalation of ions or electrons which leads to oxidation of  $\text{Ni}^{2+}$  to  $\text{Ni}^{3+}$ .

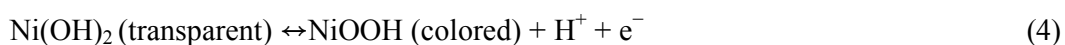
On the negative sweep, the reduction peak is associated with the extraction of ions which leads to reduction of  $\text{Ni}^{3+}$  to  $\text{Ni}^{2+}$ . The redox process in the CV curve is attributed to the following electrochemical reactions<sup>3,19</sup>:



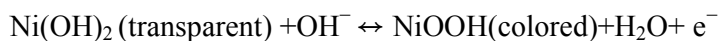
or



and



or



The cathodic and anodic peak currents of the NH-film are much higher than those of CBD and N-films. It indicates that the amount of protons and electrons incorporated into the NH-films are much higher than the others, which leads to higher electrochemical activity. This might be influenced by the porous NiO film serving as the substrate, the NH-film contains two kinds of NiO materials. As the

electrochemical reaction proceeds, two kinds of NiO materials associate with the intercalation of ions or electrons. The reversibility of the electrode reaction can be measured by the difference potential separation ( $\Delta E$ ) between the oxidation potential (anodic peak potential,  $E_O$ ) and the reduction potential (cathodic peak potential,  $E_R$ ). It can be referred from the results in Table 1 that the N-film exhibits smallest  $\Delta E$  (0.27) between the oxidation peak and the reduction peak. It indicates that N-film has best reaction reversibility, while the  $\Delta E$  (0.47) of NH-film is smaller than CBD film (0.63), which suggests that the film exhibits better reaction reversibility than the CBD film. It implies that the combination of NiO nanoparticles makes the hybrid NH-film have weaker polarization and better reaction reversibility.

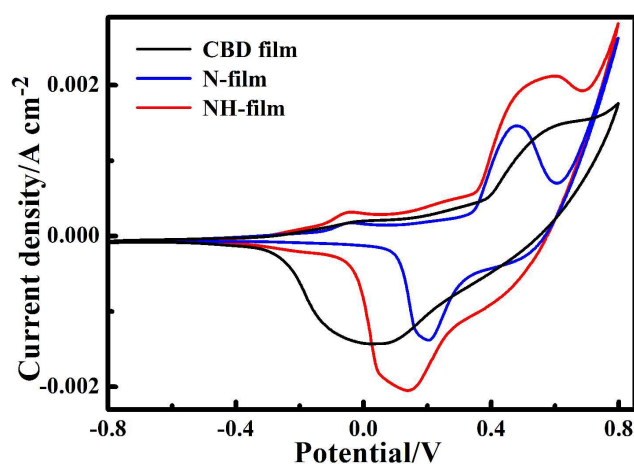


**Fig. 7** The 10th cyclic voltammograms for NiO thin films with different nanostructures

Switching speed of NiO film under alternating potentials from colored state to bleached state is of great importance to determine its practical applications in electrochromic systems. The time required for the anodic/cathodic current ( $i_O/i_R$ ) to achieve a steady state level is defined as the response time for coloration ( $t_c$ ) and bleaching ( $t_b$ )<sup>20</sup>. In this study, the CA was employed by stepping the voltages between 0.8 V and -0.8 V to examine the switching speed of the different NiO thin films. Distinct color changes can be observed during the measurement. Fig. 8 illustrates the CA curves of NiO films with different nanostructures, and the switching speed were summarized in Table 1. The results reveal that the switching time of full coloration and bleaching for the CBD film is about 3.4 s and 2.6 s respectively. For the N-film, the switching time is 1.2 s and 0.8 s, which is faster than CBD film. In contrast the switching speed of NH-film is 2.6 s and 1.6 s, which is situated between the CBD film and N-film. The reaction kinetics of counter ion migrating into the electrochromic

NiO film influenced the switching speed<sup>7, 21, 21</sup>. These results demonstrate that the hybrid film has quicker reaction kinetics, which is better than CBD NiO film.

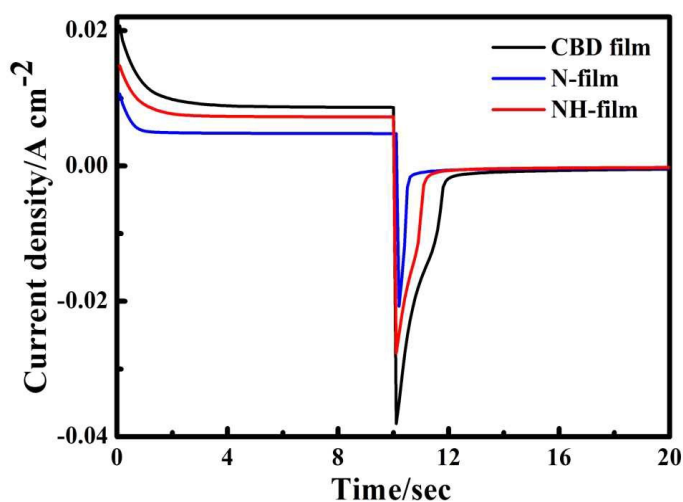


**Fig. 8** Chronoamperometric curves of different NiO films.

The electrochromic and electrochemical properties parameters of different NiO films are outlined in Table 1. Table 1 illustrates that the unique NH-film exhibits a good electrochromic performance including fast switch speed (around 2s) and high color contrast (69.4%) in company with excellent electrochemical properties compared with other two films.

**Table 1** Electrochromic and electrochemical properties parameters of different NiO films.

Sample	$\Delta T$ %	$\Delta OD$	$E_O$ (V)	$E_R$ (V)	$\Delta E$	$i_O$ (mA/cm <sup>2</sup> )	$i_R$ (mA/cm <sup>2</sup> )	Response time $t_c/t_b$ (s)
CBD film	62.9	0.64	0.65	0.02	0.63	1.5	-1.4	3.4/2.6
N-film	43.3	0.45	0.48	0.21	0.27	1.4	-1.46	1.2/0.8
NH-film	69.4	0.90	0.61	0.14	0.47	2.1	-2.2	2.6/1.6

NiO films with different nanostructures were characterized by CA using the same alternating square potentials to analyze their electrochemical stability. Fig. 9 presents the evolution of peak currents during the CA cycles. The peak currents of CBD film degrade quickly during the test process. Furthermore, the film would fall off from the ITO substrate and hardly switched from brown to transparent after 400 cycles. In contrast, the peak currents of NH-film maintain 90% of the highest values after 1000 cycles as well as the N-film (97% after 1000 cycles). It indicates that the combination

of NiO nanoparticles promote the cycling durability of the NH-film, which also corresponds with the CV measurements (Fig. 7). The excellence of electrochemical stability of the NH-film could be possibly attributed to the protection of NiO nanoparticles. The existence of NiO nanoparticles could play the role of the buffer for volumetric change of the nanowall structure. Furthermore, the NiO nanoparticles which adhered to the nanowalls may reduce internal strain and accommodate the vast volume changes. Our conclusion is that the combination of porous NiO nanowalls and NiO nanoparticles certainly contribute to the improvement of electrochromic and electrochemical performance.

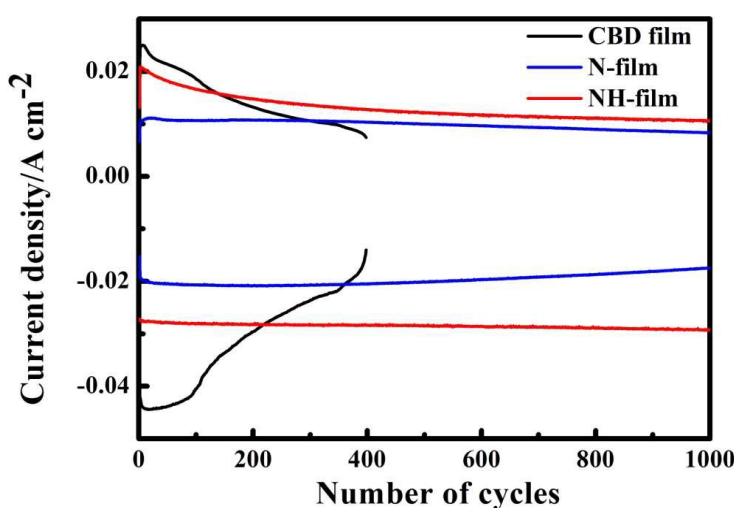


**Fig. 9** Peak current evolutions of NiO films measured during the CA cycles.

## Conclusions

CBD film and N-film have been synthesized on ITO glass by CBD method and dip coating method at room temperature in combination with a following heat-treatment process, respectively. Nanocrystalline modified nanocomb hybrid NiO film (NH-film) which was fabricated by dip coating NiO nanoparticles on CBD NiO nanowall network on ITO glass in combination with a following heat-treatment process. Large-scale production of NiO films can be easily prepared by this method. The structural, electrochromic and electrochemical properties of films are surveyed using various measurements. In this study, it turns out that the NH-film which adhered by a multitude of NiO nanoparticles showed a notable transmittance change (69.4%) as compared with CBD NiO film (62.9%) and N-film (43.3%). The response time fell in

between the N-film and CBD film. During the CV and CA measurements, the NH-film illustrated better reaction activity and cycling stability. Compared to the other two films, the NH-film exhibits weaker polarization, higher color contrast, better reactivity and cycling performance. The decoration of the NiO nanoparticles of NH-film is responsible for the enhanced electrochromic performance.

### Acknowledgements

This work was supported by the Foundation on the Creative Research Team Construction Promotion Project of Beijing Municipal Institutions, the Beijing Municipal Commission of Education Foundation (No. KM201410005015), the Rixin Training Support Project of Beijing University of Technology, the Importation and Development of High-Caliber Talents Project of Beijing Municipal Institutions (CIT&TCD 201504019), the National Natural Science Foundation of China (51302081, 61575010, 61574009, 11274028, 11574014), Beijing Nova Program (Z141109001814053) and the Science and Technology Commission of Beijing Municipality (Z151100003315018, Z151100003515004).

### References:

1. R. Ostermann and B. Smarsly, *Nanoscale*, 2009, **1**, 266-270.
2. C. G. Granqvist, E. Avendaño and A. Azens, *Thin Solid Films*, 2003, **442**, 201-211.
3. X. H. Xia, J. P. Tu, J. Zhang, X. L. Wang, W. K. Zhang and H. Huang, *Solar Energy Materials and Solar Cells*, 2008, **92**, 628-633.
4. D. S. Dalavi, R. S. Devan, R. S. Patil, Y.-R. Ma, M.-G. Kang, J.-H. Kim and P. S. Patil, *Journal of Materials Chemistry A*, 2013, **1**, 1035-1039.
5. E. Avendaño, L. Berggren, G. A. Niklasson, C. G. Granqvist and A. Azens, *Thin Solid Films*, 2006, **496**, 30-36.
6. M. R. J. Velevska, *Solar Energy Materials and Solar Cells*, 2002, **73**, 131-139.
7. B. Zhao, X. Zhang, G. Dong, H. Wang and H. Yan, *Ionics*, 2015, **21**, 2879-2887.
8. F. Cao, G. X. Pan, X. H. Xia, P. S. Tang and H. F. Chen, *Electrochimica Acta*, 2013, **111**, 86-91.
9. G. Cai, X. Wang, M. Cui, P. Darmawan, J. Wang, A. L.-S. Eh and P. S. Lee, *Nano Energy*, 2015, **12**, 258-267.
10. L. Zhao, G. Su, W. Liu, L. Cao, J. Wang, Z. Dong and M. Song, *Applied Surface Science*, 2011, **257**, 3974-3979.
11. N. Penin, A. Rougier, L. Laffont, P. Poizot and J. M. Tarascon, *Solar Energy Materials and Solar Cells*, 2006, **90**, 422-433.
12. P. S. P. L.D. Kadam, *Solar Energy Materials and Solar Cells*, 2001, **68**, 361-369.
13. K. K. Purushothaman and G. Muralidharan, *Solar Energy Materials and Solar Cells*, 2009, **93**, 1195-1201.
14. X. H. Xia, J. P. Tu, J. Zhang, X. L. Wang, W. K. Zhang and H. Huang, *Electrochimica Acta*, 2008,

- 53, 5721-5724.
15. J.-h. Zhang, G.-f. Cai, D. Zhou, H. Tang, X.-l. Wang, C.-d. Gu and J.-p. Tu, *Journal of Materials Chemistry C*, 2014, **2**, 7013.
  16. Y. C. Nikhil R. Jana, and Xiaogang Peng, *Chemistry of Materials*, 2004, **16**, 3931-3935.
  17. D. Ma, G. Shi, H. Wang, Q. Zhang and Y. Li, *Nanoscale*, 2013, **5**, 4808-4815.
  18. S. I. Cho, R. Xiao and S. B. Lee, *Nanotechnology*, 2007, **18**, 405705.
  19. M.-S. Wu and C.-H. Yang, *Applied Physics Letters*, 2007, **91**, 033109.
  20. G. Cai, J. Tu, D. Zhou, L. Li, J. Zhang, X. Wang and C. Gu, *The Journal of Physical Chemistry C*, 2014, **118**, 6690-6696.
  21. G. F. Cai, J. P. Tu, J. Zhang, Y. J. Mai, Y. Lu, C. D. Gu and X. L. Wang, *Nanoscale*, 2012, **4**, 5724-5730.
  22. B. Zhao, S. Lu, X. Zhang, H. Wang, J. Liu, H. Yan, *Ionics*, 2015, 10.1007/s11581-015-1547-3.